Inhibitors of the Molybdenum Cofactor Containing 4-Hydroxybenzoyl-CoA Reductase[†]

Jörg Johannes,[‡] Mihaela-Carmen Unciuleac,[§] Thorsten Friedrich,[||] Eberhard Warkentin,[⊥] Uli Ermler,[⊥] and Matthias Boll*,[‡]

Institute of Biochemistry, University of Leipzig, D-04103 Leipzig, Germany, Molecular Biology Program, Sloan-Kettering Institute, New York, New York 10065, Institute of Organic Chemistry and Biochemistry, University of Freiburg, Freiburg, Germany, and Max-Planck-Institute for Biophysics, Frankfurt, Germany

Received January 24, 2008; Revised Manuscript Received February 25, 2008

ABSTRACT: 4-Hydroxybenzoyl-CoA reductase (4-HBCR) is a member of the xanthine oxidase (XO) family of molybdenum cofactor containing enzymes and catalyzes the irreversible removal of a phenolic hydroxy group by reduction, yielding benzoyl-CoA and water. In this work the effects of various activity modulating compounds were characterized by kinetic, electron paramagnetic resonance (EPR) spectroscopic, and X-ray crystallographic studies. 4-HBCR was readily inactivated by cyanide and by the reducing agents titanium(III) citrate and dithionite; in contrast, reduced viologens had no inhibitory effect. Cyanide inhibition occurred in both the oxidized and reduced state of 4-HBCR. In the reduced state, cyanide-inhibited 4-HBCR was reactivated by simple oxidation. In contrast, reactivation from the oxidized state was only achieved in the presence of sulfide. Dithionite-inhibited 4-HBCR was reactivated by oxidation, whereas inhibition by titanium(III) citrate was irreversible. The previously reported inhibitory effect of azide could not be confirmed; instead, azide rather protected the enzyme from inactivation by titanium(III) citrate. The EPR spectra of the Mo(V) states were nearly identical in the noninhibited methyl viologen and in the dithionite-inhibited states of 4-HBCR; they exhibited a hyperfine splitting due to magnetic coupling with two solvent-exchangeable protons. The cyanide-treated enzyme showed the typical desulfo-inhibited Mo(V) EPR signal in D_2O, whereas in H_2O the hyperfine splitting was altered but indicated no loss of Mo(V)−proton interactions. The structures of dithionite- and azide-bound 4-HBCR were solved at 2.1 and 2.2 Å, respectively. Both dithionite and azide bound directly to equatorial ligation sites of the Mo atom. The results obtained revealed further insights into the active site of an unusual member of the XO family of molybdenum cofactor containing enzymes.

In the catabolism of aromatic compounds in anaerobic bacteria many unprecedented reactions have been revealed in recent years (*1–4*). A unique reaction of this metabolism is catalyzed by 4-hydroxybenzoyl-CoA reductase (4-HBCR).[1] It involves the removal of the phenolic hydroxy group of the substrate by two-electron reduction, yielding water and benzoyl-CoA; a reduced ferredoxin serves as electron donor for 4-HBCR (Figure 1). The reaction catalyzed by 4-HBCR plays an important role in the anaerobic degradation of phenolic compounds such as phenol, *p*-cresol, or low molecular mass aromatic products derived from lignin degradation. The oxygen-sensitive 4-HBCR has so far only been isolated from the denitrifying *Thauera aromatica* (*5, 6*). It belongs to the xanthine oxidase (XO) family of molybdenum cofactor containing enzymes. Accordingly, the 270 kDa enzyme has a $(\alpha\beta\gamma)_2$ subunit architecture and harbors a molybdopterin cytosine dinucleotide cofactor, two [2Fe-2S]$^{+1/+2}$clusters, one FAD, and an additional [4Fe-4S]$^{+1/+2}$ cluster per heterotrimer (*6–8*).

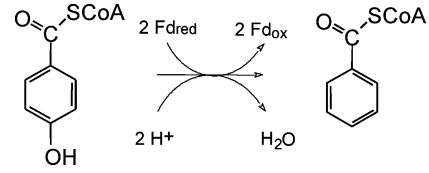

FIGURE 1: Reaction catalyzed by 4-HBCR. Fd = ferredoxin.

Enzymes of the XO family typically catalyze oxygen atom transfer reactions (usually the hydroxylation of the substrate with water) at an active site Mo atom that acts as a Lewis acid and redox carrier (*9–11*). Reducing equivalents are transferred from the substrate via the Mo cofactor and the two [Fe-2S]$^{+1/+2}$ clusters and in some cases via a flavin cofactor to external electron acceptors. In contrast, 4-HBCR is the only XO family member which catalyzes the irreversible reduction of the substrate. In recent years some unique properties of 4-HBCR among XO family enzymes were assigned to the unusual reaction catalyzed, which are briefly summarized in the following.

[†] This work was supported by the German Research Council (BO 1565/5-2) and the Max-Planck-Gesellschaft.

* Corresponding author. Phone: +49-341-9736996. Fax: +49-341-9736910. E-mail: boll@uni-leipzig.de.

[‡] University of Leipzig.

[§] Sloan-Kettering Institute.

[||] University of Freiburg.

[⊥] Max-Planck-Institute.

[1] Abbreviations: 4-HBCR, 4-hydroxybenzoyl-CoA reductase; 4-OH-BCoA, 4-hydroxybenzoyl-CoA; XO, xanthine oxidase.

10.1021/bi800137v CCC: $40.75
Published on Web 04/05/2008

(i) In comparison to other XO family enzymes such as XO, quinoline oxidase (QOR), or isoquinoline oxidase, the substrate of 4-HBCR is not a heterocycle but a homocyclic aromatic CoA ester. As a consequence the catalytic mechanism of 4-HBCR reduction cannot be described by a simple reversal of the reaction cycle proposed for other enzymes of the XO family. Instead, a mechanism according to an enzymatic Birch reduction involving radical intermediates has been proposed (*12, 13*). (ii) Reduction of 4-hydroxybenzoyl-CoA (4-OH-BCoA) requires much lower electrochemical potentials of the redox carriers than for the reactions catalyzed by other XO family members. In accordance, the redox potentials of the Mo cofactor, the [4Fe-4S] cluster, and the flavin cofactor are unusually low, and the enzyme is sensitive to oxygen (*5, 7*). (iii) The irreversible electron transfer from the donor to the substrate suggested a special arrangement of the five redox cofactors. The recently solved structure of 4-HBCR showed an electron transfer chain over a distance of 55 Å as follows: reduced ferredoxin → [4Fe-4S] → FAD → [2Fe-2S] I → [2Fe-2S] II → Mo cofactor → substrate. Electron transfer rate calculations indicated that the unusually high distance between the [4Fe-4S] cluster and FAD (16.5 Å) favors the unidirectional electron transfer from the external electron donor reduced ferredoxin to the Mo-bound substrate (*14*).

The molybdenum atom in XO family enzymes is usually coordinated by two dithiolene sulfur ligands of the pyranopterin cofactor, one oxo, one sulfo, and a hydroxy or water ligand in square-pyramidal geometry (*9–11*). The sulfur ligand is essential for catalysis, but there was much debate about its position in the coordination sphere of the Mo atom. While the recently solved structures from bovine milk xanthine dehydrogenase (*15*) and QOR (*16*) clearly indicated an equatorial position, the structure obtained from "resulfurated" crystals of aldehyde oxidoreductase from *Desulfovibrio gigas* revealed an apical position (*17*). It remains unclear whether the latter was an artifact or a special property of XO family enzymes from sulfate-reducing bacteria (*9, 18*).

The recently solved structure of 4-HBCR did not indicate the presence of a sulfur ligand at the Mo atom (*14*). However, like other members of the XO family, 4-HBCR was inhibited by cyanide (*5*). Cyanide inhibition has been assigned to the release of the sulfur ligand from the Mo cofactor as thiocyanate, thereby inactivating the enzyme (*10, 19*). Thus, 4-HBCR was suggested to be crystallized in an inactive desulfo state. Surprisingly, it has been reported that 4-HBCR was also inhibited by azide, which has not been described for any other member of the XO family so far (*5*).

In this work we characterized known and novel inhibitors/effectors of 4-HBCR by kinetic, EPR spectroscopic, and X-ray crystallographic studies. The results obtained revealed further unique properties of 4-HBCR within the family of XO enzymes.

EXPERIMENTAL PROCEDURES

Growth of Bacterial Cells. T. aromatica strain K172 (DSMZ 6984) was grown anaerobically at 30 °C in a mineral salt medium in a 200 L fermenter with 4-hydroxybenzoate and nitrate in a molar ratio of 1:3.5 as sources of energy and cell carbon. Continuous feeding of the substrates, cell harvesting, storage, and preparation of cell extracts were carried out as described earlier (*5*).

Protein Purification and Sample Storage. Purification of 4-HBCR from extracts of *T. aromatica* was performed under strictly anaerobic conditions as described earlier (*5*). The procedure included three chromatographic steps using anion-exchange chromatography on DEAE-Sepharose, Hi Load Q-Sepharose (GE Healthcare, each), and chromatography on Cibacron Blue agarose (Sigma). Concentration of the protein samples was achieved by centrifugation (3000 *g*) in Vivaspin 6 microconcentrators (exclusion limit 50 kDa). The purity of these enzyme preparations was >90% as estimated by Coomassie staining of SDS gels. Sixty milligrams of enriched 4-HBCR was maximally obtained from 200 g of cells (wet mass) with specific activities of 3−5 μmol of 4-OH-BCoA reduced min^{-1} mg^{-1}. Concentrated protein samples were shock frozen and stored in liquid nitrogen for several months without loss of activity.

Synthesis and Purification of 4-OH-BCoA. 4-OH-BCoA was synthesized enzymatically from CoA and 4-hydroxybenzoic acid using partially purified 4-OH-benzoate CoA ligase from *T. aromatica* (*20*). Purification and purity control were carried out by HPLC analysis as described earlier (*21*).

Enzyme Assays. Activity of 4-HBCR was determined in two different assays. The spectrophotometric assay followed the oxidation of reduced methyl viologen as described earlier (*7*). It contained 50 mM potassium phosphate buffer, pH 7.0, 2.5 mM $MgCl_2$, 1 mM methyl viologen reduced with dithionite to $A_{730} = 1.6–1.8$ ($\varepsilon_{MVred(730nm)} = 2400\ M^{-1}\ cm^{-1}$), and 0.2 mM 4-OH-BCoA. With titanium(III) citrate or dithionite as electron donor a discontinuous assay was applied that followed substrate consumption and product formation by HPLC analysis. The typical assay for HPLC analysis contained 50 mM potassium phosphate buffer, pH 7.0, 2.5 mM $MgCl_2$, 1 mM titanium(III) citrate or 2 mM dithionite, and 0.2 mM 4-OH-BCoA in a final volume of 350 μL. Aliquots of 50 μL were taken at 0.5, 1, 2, and 4 min, added to 100 μL of methanol, and centrifuged in an Eppendorf centrifuge for 15 min at 4 °C. From the supernatant, 50 μL were applied to HPLC analysis on a Waters 2695 chromatography system with a Waters 2996 photodiode array detector. Separation was by a Eurospher RP C18 column (250 × 4.6 mm; Knauer, Berlin, Germany) with a gradient of acetonitrile in 50 mM aqueous potassium phosphate, pH 6.8, at a flow rate of 0.75 mL min^{-1}. The gradient applied was the following: 0−7 min, 10−25% acetonitrile; 7−8 min, 25−40% acetonitrile; 8−10 min, 40% acetonitrile; 10−11 min, 40−10% acetonitrile; 11−15 min, 10% acetonitrile. Retention times were 7.2 min for 4-OH-BCoA and 8.8 min for benzoyl-CoA, respectively. Detection was carried out at 260 nm. The amount of CoA esters formed was calculated by comparison of the peak areas with standards of 4-OH-BCoA and benzoyl-CoA. The detection limit was 1 μM CoA ester.

Sample Preparation. All sample preparations were carried out under strictly anaerobic conditions in an anaerobic glovebox (Coy Laboratory Systems) under an N_2/H_2 atmosphere (95:5 v/v). Oxidized enzyme (4-$HBCR_{ox}$) was freshly prepared by incubation with an excess of an anaerobically prepared saturated thionine stock solution (approximately 10 mM in 20 mM TEA and 2.5 mM $MgCl_2$, pH 7.8, referred to as buffer A). The enzyme was fully oxidized when the added

thionine solution did not lose color over 30 min at 20 °C. Oxidant and salt were quantitatively removed by passing the enzyme over a Sephadex G-25 column (PD-10; GE Healthcare), which had been equilibrated with buffer A. 4-$HBCR_{ox}$ was stable over 24 h under anaerobic conditions at room temperature.

Inactivation by Cyanide. For incubation of 4-$HBCR_{ox}$ with cyanide 8.8 mg of enzyme in 1 mL of buffer A was incubated with 5 mM potassium cyanide for different time points up to 20 h. Excess cyanide was removed by desalting using a PD-10 column equilibrated in buffer A. 4-HBCR was considered to be in the cyanide-inhibited state (4-$HBCR_{cn}$) when residual activity was less than 0.01 μmol of 4-OH-BCoA reduced min^{-1} mg^{-1}. 4-$HBCR_{cn}$ was frozen and stored in liquid nitrogen for further use.

Inactivation by Reducing Agents. 4-$HBCR_{ox}$ preparations in buffer A (2 mg mL^{-1}) were supplemented with varying amounts of reducing agents [titanium(III) citrate, dithionite, dithionite-reduced methyl viologen, and benzyl viologen]. All experiments were carried out under strictly anaerobic conditions in glass vials sealed with rubber stoppers at 20 °C. Addition of reducing agents and withdrawal of samples were carried out with gas-tight syringes (Hamilton). In the case of the viologens, 200 mM anaerobically oxidized stock solutions were reduced by dithionite to maximal 50 mM reduced viologen dye in the glovebox. Under these conditions it was guaranteed that all dithionite added was completely oxidized to sulfite in the course of viologen dye reduction.

Reconstitution of Activity by Sulfide. Three different assays were used for testing the mode of reconstitution of inhibited 4-HBCR.

(1) Assay A. 4-$HBCR_{ox/cn}$ was transferred into 100 mM sodium pyrophosphate, pH 8.0 (buffer B), by passage through a PD-10 column. Sodium sulfide was added at room temperature to final concentrations of 2 and 5 mM. Samples were taken at different time intervals from the reaction assay and tested for activity. After 1 h incubation, Na_2S was removed by passing the assay mixture (300–400 μL) through a PD-10 column equilibrated in buffer A and tested for activity.

(2) Assay B. For determination of the concentration dependency, varying amounts of Na_2S (25 μM up to 5 mM) were added to the activity assay without preincubation of 4-$HBCR_{ox/cn}$. For this purpose, the enzyme was preincubated in cuvettes for 1 min at 30 °C; then the reaction was started by addition of substrate.

(3) Assay C. 4-$HBCR_{ox/cn}$ (2 mg) was anaerobically preincubated with 5 mM Na_2S in the spectrophotometric activity assay mixture for 1 min at 30 °C (450 μL) after which the substrate was added. After completion of the reaction, the activity of reactivated 4-HBCR was then tested in the spectrophotometric assay. To test whether such a reactivated 4-HBCR preparation was stable, all reactants of the spectrophotometric assay were removed by gel filtration on a PD-10 column equilibrated in buffer A, and activity was measured again.

Determination of Thiocyanate. Thiocyanate (SCN^-) was assayed according to the method of Westley (*22*). For this purpose, 1 mL of 4-$HBCR_{ox}$ (37 μM) and, as a reference, milk XO (12 μM, purified according to the procedure described (*23*); specific activity was 2.7 μmol min^{-1} mg^{-1}) were incubated with 5 mM KCN for 20 h as described above and concentrated using a Vivaspin concentrator (Sartorius, Göttingen, Germany) with 50 kDa cutoff. Then, 250 μL of the flow-through was added to 250 μL of Sorbö's reagent [10 g of $Fe(NO_3)_3$ dissolved in 20 mL of 65% HNO_3, diluted to 150 mL with distilled water] and incubated for 5 min at 20 °C in a quartz cuvette sealed with parafilm. After incubation, the visible spectrum was recorded from 350 to 700 nm against buffer A treated in the same way. Quantification was by the absorption maximum of $Fe(SCN)_3$ at 460 nm against a calibration curve from 4 to 200 μM KSCN in buffer A (ε_{460} = 2000 M^{-1} cm^{-1}; our determination). The detection limit was 4 μM KSCN in buffer A. XO from bovine milk treated in the same way yielded 1.16 mol of SCN^-/mol of enzyme.

EPR Sample Preparation and Measurement. 4-$HBCR_{ox}$ (245 μL, 15−30 mg mL^{-1} in buffer A) was anaerobically mixed with 5 μL of an anaerobic stock solution of 100 mM dithionite, 100 mM reduced methyl viologen, or 50 mM titanium(III) citrate, yielding final concentrations of 2 and 1 mM of reductant, respectively. Samples were transferred into X-band EPR tubes using a Teflon tube mounted on a syringe and frozen in liquid nitrogen 2 min after mixing. 4-$HBCR_{az}$ was prepared by adding 5 μL of 250 mM NaN_3 to 240 μL of concentrated 4-$HBCR_{ox}$, followed by incubation for 30 min at 20 °C. The enzyme was subsequently reduced by adding 5 μL of 50 mM reduced methyl viologen as described above. 4-$HBCR_{D_2O}$ and 4-$HBCR_{D_2O/cn}$ were prepared by passing 4-$HBCR_{ox}$ and 4-$HBCR_{ox/cn}$ over a PD-10 column equilibrated in buffer A prepared with D_2O. After incubation for 1 h at 20 °C, the samples were passed over the freshly equilibrated PD-10 columns again. Samples were subsequently concentrated and further prepared as above.

EPR measurements were conducted with a Bruker EMX 1/6 spectrometer operating at X-band (9.2 GHz). The sample temperature was controlled with an Oxford Instrument ESR-9 helium-flow cryostat. The magnetic field was calibrated using a strong or a weak pitch standard. Typical EPR parameters were as follows: microwave frequency, 9.462 GHz; power, 2 mW; modulation frequency, 100 kHz; modulation amplitude, 0.2 mT; and temperature, 80 K. Simulations of spectra were carried out using the WINEPR software package (Bruker).

Crystallization of 4-HBCR. Crystallization of 4-HBCR was carried out under the conditions described previously (*14*). For additional soaking experiments isolated crystals were treated with freshly prepared anaerobic 2 mM sodium dithionite as well as 5 mM sodium azide and subsequently frozen. Data were collected at the ID29 beamline at the ESRF in Grenoble and processed with the HKL software (*24*) and programs of the CCP4 suite [CCP4 (*25*)]. The determined cell axis indicated that the crystals belong to crystal form 1 (*26*), and the rapid decrease of the R and R_{free} factors during refinement with REFMAC (*27*) confirmed this assumption. Molecular graphic studies were performed with O (*28*) and COOT (*29*). Dithionite ($S_2O_4^{2-}$) and azide (N_3^-) were incorporated into the polypeptide model in several conformations and the results analyzed. The quality of the structure was assessed with PROCHECK (*29*).

RESULTS

In the first report about the isolation and preliminary characterization of 4-HBCR, the enzyme was shown to be

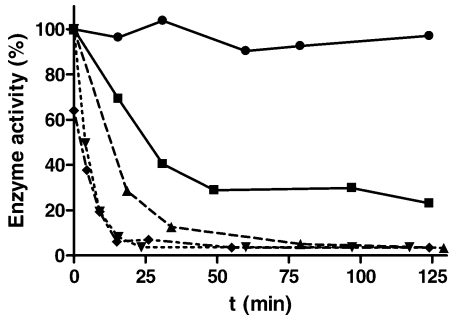

FIGURE 2: Inactivation of 4-HBCR$_{ox}$ by sodium dithionite. 4-HBCR$_{ox}$ was incubated with 0.2 mM (■), 1 mM (▲), 2 mM (▼), 5 mM (◆), and without (●) sodium dithionite. Activity was tested at the indicated time points.

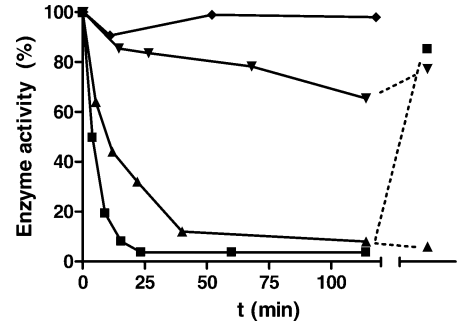

FIGURE 3: Effects of different reducing agents on 4-HBCR activity. Incubation of 4-HBCR$_{ox}$ with 2 mM sodium dithionite (■), 2 mM titanium(III) citrate (▲), 2.5 mM reduced methyl viologen (▼), and 2.5 mM reduced benzyl viologen (◆). After 120 min, the inactivated samples were oxidized with thionine and tested for activity.

inhibited by oxygen, cyanide, and, unexpectedly, azide (*5*). However, the mode of inhibition was not further investigated in these studies. To understand the mechanisms of various enzyme activity effecting compounds and to draw conclusions for the overall structure/function relationship of 4-HBCR, a detailed kinetic, EPR spectroscopic, and structural study was carried out with known and novel activity inhibiting compounds. The 4-HBCR preparations investigated here are referred to as follows: 4-HBCR$_x$, with x = cn for cyanide, x = ti for titanium(III) citrate, x = dit for dithionite, and x = az for azide-treated 4-HBCR; x = ox refers to thionine oxidized and x = red to methyl viologen reduced 4-HBCR.

Kinetic Studies. (A) Effect of Reducing Agents. 4-HBCR was reported to be irreversibly inactivated by oxygen with $t_{1/2}$ = 17 min (*5*). For this reason, purification and storage of the enzyme have generally been carried out in an anaerobic glovebox in the presence of dithionite (0.1 mM). However, we observed that increasing amounts of dithionite did not further protect the enzyme from oxygen damage but rather exhibited an inhibitory effect. To test this in more detail, the time- and concentration-dependent inactivation by dithionite was investigated (Figure 2).

When kept under strictly anoxic conditions in a glovebox, no significant loss of 4-HBCR$_{ox}$ activity was observed within 48 h. In contrast, 4-HBCR$_{dit}$ was inactivated in a time- and concentration-dependent manner (Figure 2). Thus, the protective effect of dithionite could not be confirmed, and dithionite rather appeared to inhibit 4-HBCR. Sodium sulfite (2 mM) had no inhibitory effect on 4-HBCR$_{ox}$, which excludes that the oxidization product of dithionite was the 4-HBCR-inhibiting compound.

To test whether inhibition was specific for dithionite or whether 4-HBCR was generally sensitive to reduction, the reductants titanium(III) citrate and reduced methyl and benzyl viologen were tested as potential inhibitors at 2–2.5 mM concentrations. In the presence of titanium(III) citrate, 4-HBCR was inactivated in a time-dependent manner with a slightly decreased inhibitory efficiency when compared to the effect of dithionite (Figure 3). Incubation with 2 mM sodium citrate or 2 mM titanium(IV)/citrate [prepared by air oxidation of titanium(III) citrate] had no effect on 4-HBCR, suggesting that indeed the titanium(III) citrate complex is the true inhibiting compound. The inhibitory effect of reduced methyl viologen was negligible and most probably due to some traces of residual dithionite, which was generally used for methyl viologen reduction; reduced benzyl viologen did not inhibit the enzyme at all.

For testing the reversibility of the inhibitory effect of dithionite, 4-HBCR$_{dit}$ was anaerobically oxidized by addition of excess thionine. As shown in Figure 3, 85–90% of the activity of dithionite-inactivated enzyme was restored by this procedure. 4-HBCR$_{dit}$ could even be reactivated to 90% of the original activity by exposure to air for a few minutes (not shown). In these experiments 4-HBCR was inactivated again by oxygen after prolonged incubation (>10 min). In contrast, the inhibitory effect of titanium(III) citrate was not reversed by oxidation with thionine or air. The latter finding confirms that 4-HBCR was not simply inhibited by reduction but rather by specific and differing mechanisms of inhibition in the case of dithionite and titanium(III) citrate. In summary, 4-HBCR appears to be sensitive to both oxidation and reduction, with the inhibitory effect strongly depending on the nature of the oxidant/reductant used. As so far dithionite was commonly used as the reductant for studies with 4-HBCR, the effect of activity-modulating compounds was reinvestigated and described in the following.

(B) Effect of Cyanide. Enzymes of the XO family are generally inactivated by cyanide, which is usually accompanied by the release of a sulfur ligand from the Mo cofactor of the enzyme as thiocyanate (*10*). In a previous study, 4-HBCR reduced by 0.1 mM dithionite was also found to be irreversibly inactivated by 0.1 mM cyanide in a pseudo-first-order reaction (*5*). We reinvestigated inhibition of reduced and oxidized 4-HBCR by cyanide by varying the inhibitor concentration. 4-HBCR$_{ox}$ was readily inactivated by cyanide (Figure 4). For example, approximately 60% of the activity was lost after 1 min incubation with 0.2 mM cyanide. However, even after prolonged incubation, complete inhibition of 4-HBCR was only achieved with cyanide concentrations higher than 0.5 mM. In the methyl viologen reduced state, no significant difference of the inhibitory effect of cyanide was observed. Removal of cyanide by desalting did not result in a reactivation of 4-HBCR$_{cn}$.

The formation of thiocyanate in the course of cyanide inactivation can be determined in a radioactive or spectrophotometric assay (*22, 30*). No formation of thiocyanate could be determined by the spectrophotometric assay from 37 μM 4-HBCR$_{ox}$. In a control experiment under identical conditions bovine XO was used, and the formation of 1.16 thiocyanate/dimeric XO was determined. The substoichiometric formation of 0.58 thiocyanate/Mo cofactor of XO was

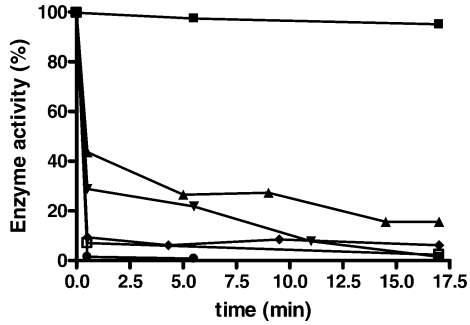

FIGURE 4: Inactivation of 4-HBCR$_{ox}$ by cyanide. Incubation of 4-HBCR$_{ox}$ with 0.2 mM (▲), 0.5 mM (▼), 1 mM (◆), and 2 mM KCN (●) and incubation of 4-HBCR$_{red}$ with 2 mM KCN (□). The control without cyanide was stable under these conditions (■).

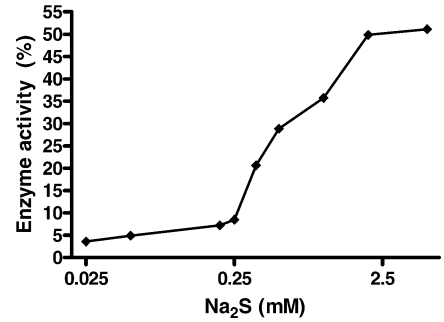

FIGURE 5: Reactivation of cyanide-inactivated 4-HBCR by sodium sulfide. 4-HBCR$_{cn/ox}$ was incubated with 25 μM−5 mM sodium sulfide for 1 min, after which activity was measured in the presence of differing amounts of sodium sulfide. Note that after removal of sodium sulfide, the enzyme remained inactive again.

in the expected range as XO preparations usually contain a varying content of "desulfurated" Mo cofactor. As a result, the mode of cyanide inactivation appeared to be different in 4-HBCR and in bovine XO.

(C) Effect of Azide. To our knowledge, 4-HBCR is the only member of the XO family that was reported to be sensitive to azide (*5*). We reinvestigated the time-dependent inhibition of 4-HBCR by azide in the thionine-oxidized and methyl viologen reduced state at 1–5 mM concentration. Even after 120 min of incubation no significant inhibition was observed versus a control sample without azide (not shown). For testing whether azide exhibits an additional inhibitory effect in the dithionite or titanium(III) citrate reduced state, 4-HBCR was incubated with 2 mM dithionite and titanium(III) citrate, respectively, in the presence and absence of 5 mM sodium azide. While the presence of azide had no effect on dithionite inhibition, the inhibitory effect of titanium(III) citrate was clearly diminished. Even after 2 h incubation with titanium(III) citrate the enzyme restored about 60% of the activity of a control without azide (not shown). Note that in the absence of azide 2 mM titanium(III) citrate resulted in a complete inhibition of 4-HBCR within 2 h (Figure 3).

(D) Reactivation of 4-HBCR by Sulfide. The reactivation of the cyanide-inhibited state by sulfide has been demonstrated for a number of molybdenum cofactor containing enzymes (*9–11, 19*). To probe such a reactivation, 4-HBCR$_{ox/cn}$ was first desalted to remove excess cyanide and was then incubated with varying sulfide concentrations (1–10 mM) for 10 min to 24 h. An aliquot of such an enzyme preparation was subsequently used for the typical spectrophotometric assay with reduced methyl viologen as electron donor. In neither case was 4-HBCR activity restored. However, when sulfide was added to the enzyme activity assay (5 mM), 4-HBCR activity could be restored up to 60% of the original activity (Figure 5). When the excess of sulfide of such a reactivated 4-HBCR preparation was removed by desalting, the activity was completely lost again, whereas the restored activity remained stable in the presence of 5 mM sulfide. In summary, reactivation of 4-HBCR$_{cn}$ by sulfide was obviously only achieved during substrate turnover and was only stable in the presence of excess sulfide.

4-HBCR$_{red/cn}$ could not be reactivated with sulfide by the procedure described above. Instead, anaerobic oxidation (e.g., by thionine) immediately restored the activity up to 99% even in the absence of sulfide. In summary, the mode of cyanide inactivation and that of reactivation by sulfide proceeded in two different redox-dependent manners.

In further studies sulfide was tested to reactivate 4-HBCR$_{dit}$ and 4-HBCR$_{ti}$ as described above for 4-HBCR$_{cn}$. Addition of 5 mM sodium sulfide to 4-HBCR$_{dit}$ and 4-HBCR$_{ti}$ did not result in any reactivation even after incubation for 10 h. Thus, inactivation of 4-HBCR by the two reductants apparently did not proceed via the elimination of the sulfur ligand from the Mo atom.

EPR Spectroscopic Studies. In a recent study the redox cofactors of 4-HBCR were characterized by EPR and Mössbauer spectroscopy (*7*). A typical EPR signal from the paramagnetic Mo(V) signal was observed in reduced 4-HBCR preparations (at redox potentials between −380 and −550 mV) and characterized (g_{x-z} = 1.99, 1.965, and 1.965; E'° Mo(VI/V) = −380 mV and E'° Mo(V/IV) = −500 mV). In this study, even during substrate turnover none of the Mo(V) EPR signals described for other members of the XO family were detected with 4-HBCR [e.g., "slow", "rapid", "very rapid", "inhibited" (*31, 32*)]. Therefore, the terminology introduced for Mo(V) EPR signals of the XO family is not applicable to 4-HBCR. The $S = {}^1/_2$ low-spin EPR signal of 4-HBCR showed a typical hyperfine splitting which was interpreted as a result of magnetic interactions between Mo(V) with one or more protons (*7*). As in these studies dithionite was used as reductant, the Mo(V) signals of enzyme preparations were reinvestigated under various conditions and characterized in more detail.

As depicted in Figure 6a,b (left panel), the Mo(V) spectra of dithionite and methyl viologen reduced 4-HBCR were nearly identical. A highly similar signal was also obtained with titanium(III) citrate (not shown). The incubation time with dithionite was chosen in such a way that 4-HBCR was completely inactivated. Obviously, the observed differences in enzyme inhibition by different electron donors were not reflected by EPR-detectable modifications of the Mo(V) EPR signal. Addition of excess 4-OH-BCoA (5 mM) to dithionite or titanium(III) citrate reduced 4-HBCR for 1 s followed by immediate freezing in an isopentane/liquid nitrogen cooling mixture resulted in a decrease of the Mo(V) signal to less than 5%, indicating that during substrate turnover the Mo is mainly in the oxidized state (not shown). Most importantly, the remaining Mo(V) signal was identical to that observed in the absence of the substrate. The Mo(V) EPR signal was also not significantly changed in the presence of sodium azide (Figure 6c, left panel). This finding was surprising as azide

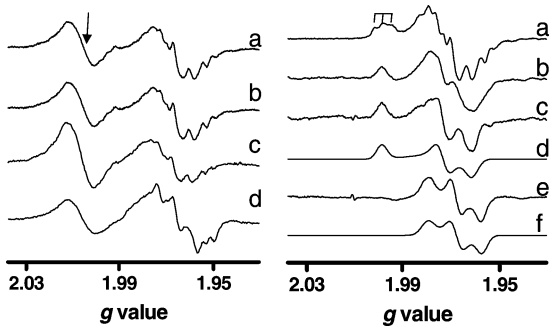

FIGURE 6: EPR spectra of 4-HBCR. Left panel: EPR spectra of 4-HBCR as isolated after (a) reduction with 2 mM dithionite and (b) 2 mM reduced methyl viologen. (c) and (d) were reduced with 1 mM reduced methyl viologen (c) after incubation with 2 mM sodium azide for 30 min and (d) after incubation with 2 mM sodium cyanide for 2 min and desalting. Right panel: For better presentation the flavin semiquinone signal at $g = 2.008$ was subtracted from all spectra. EPR spectra of 4-$HBCR_{dit}$ (a) as isolated, (b) as isolated in D_2O, (c) as isolated in D_2O after subtraction of the 4-$HBCR_{cn}$ spectrum in D_2O ($\times 0.18$), as shown in (e), (e) 4-$HBCR_{cn}$ in D_2O. (d) and (f) are simulations of the spectra in (c) and (e), respectively. The arrow in the left panel points to the FADH semiquinone radical signal; the three lines in (a) in the right panel point to the split g_z component of the Mo(V) signal. For EPR conditions see Experimental Procedures.

was shown to coordinate to the Mo atom (see below). A possible explanation is that azide does not bind to Mo(V) but rather to diamagnetic oxidation states [e.g., Mo(VI) in case of binding to 4-HBCR crystals]. Cyanide-inhibited 4-HBCR was prepared by incubating 4-$HBCR_{ox}$ with 5 mM cyanide for 20 h followed by removal of excess cyanide and reduction. The Mo(V) signal in 4-$HBCR_{red/cn}$ was significantly changed in comparison to the spectra recorded in the absence of cyanide; however, no loss of proton/Mo(V) hyperfine interaction was observed as the number of split features remained constant (Figure 6d, left panel).

We propose that the Mo(V) signal of 4-HBCR is split due to hyperfine interaction with two protons. Especially in the g_z region of the Mo(V) signal the presence of a triplet feature with a nearly 1:2:1 ratio (with $A[^1H] = 0.6$ mT) indicated a magnetic interaction of the Mo(V) species with two protons (Figure 6a, right panel). In order to further characterize the EPR properties of the Mo(V) EPR signals of noninhibited and cyanide-inhibited 4-HBCR, enzyme samples were prepared in D_2O, and the Mo(V) signals were recorded and simulated (Figure 6, right panel). The Mo(V) spectrum of 4-$HBCR_{red/D_2O}$ could not be simulated by a single $S = {}^1/_2$ species but rather was interpreted as an overlay of two different $S = {}^1/_2$ species (Figure 6b, right panel). To test whether this signal resulted from a mixture of an active and inhibited 4-HBCR species, the enzyme was completely converted into the 4-$HBCR_{ox/cn}$ state in D_2O followed by subsequent reduction. The resulting 4-$HBCR_{red/D_2O/cn}$ species exhibited the typical $S = {}^1/_2$ EPR spectrum of the so-called desulfo-inhibited state of XO family enzymes (*18, 31, 33*) (Figure 6e). The spectrum could be simulated with $g_{xyz} =$ 1.9795, 1.968, and 1.957 and line widths = 0.92, 0.78, and 0.77 mT, respectively (Figure 6f). The difference spectrum of the Mo(V) spectrum 4-$HBCR_{red/D_2O}$ minus 4-$HBCR_{red/D_2O/cn}$ ($\times 0.18$) gave a nearly pure $S = {}^1/_2$ EPR signal, which could be simulated with $g_{xyz} = 1.9984$, 1.9735, and 1.9617 and line widths = 0.82, 0.86, and 0.9 mT, respectively (Figure 6c and Figure 6d). This spectrum is interpreted as the noninhibited Mo(V) signal of 4-HBCR. The ratio between the noninhibited/desulfo-inhibited Mo(V) EPR signal in 4-HBCR preparations as isolated was 5.5:1 as estimated by integration of the individual signals. Due to the presence of a mixture of two different 4-HBCR species the hyperfine splitting of the Mo(V) EPR signal in H_2O could not be simulated in an accurate way.

Structures of 4-HBCR in the Presence of Dithionite and Azide. In a previous study the structure of 4-HBCR was determined from crystals that were anaerobically grown from 4-$HBCR_{dit}$ and 4-$HBCR_{dit/cn}$ (*14, 26*). Both structures including Mo ligation were essentially identical. Since crystal growth took several weeks, the dithionite added to the enzyme preparation for crystallization trials was considered to be completely oxidized. The Mo atom in the structures of 4-HBCR was coordinated by two sulfur ligands from the dithiolene group of the cofactor, two oxo, and one water or hydroxy ligand (Figure 7a). A sulfur ligand was not found, indicating that the structure was determined in the most possibly desulfurated state.

In this work crystals were grown under the established conditions and soaked successfully with two compounds that modulate activity: sodium dithionite and sodium azide. After data collection and refinement the R_{free} value converged to 22.6% and 22.8% for the 4-$HBCR_{dit}$ (resolution range 30–2.1 Å) and 4-$HBCR_{az}$ (resolution range 30–2.18 Å) structures. Their overall structures and the structure determined previously (*14*) were essentially identical, documented by rms deviations of 0.4 and 0.5 Å, respectively. Significant residual electron density higher than 8σ (4-$HBCR_{dit}$) and 7σ (4-$HBCR_{az}$) was solely detected within the ligation sphere of the Mo atom of the molybdopterin cofactor (Figure 7), which is interpreted as binding of dithionite and azide. In both structures extra electron density was only positioned at the spatially adjacent equatorial oxygen ligation sites of the native enzyme and beyond them (Figure 7). Therefore, the apically located oxygen and the equatorially located sulfurs of the dithiolene group were not affected from binding of the soaked compounds. The electron density of the ligands was difficult to interpret on an atomic level due to the following reasons: (i) the presence of a ligation mixture due to the partial occupancy of 4-HBCR with dithionite and azide, (ii) their variable binding mode, (iii) the proximity to the strongly scattering Mo atom, and (iv) the limited resolution of the crystals.

Modeling of the extra electron density in 4-$HBCR_{dit}$ revealed the most convincing fit by positioning the dithionite molecule to the Mo atom in a manner such that the bond between the two sulfur atoms runs parallel to the line connecting the two equatorial oxygen atoms of the native structure. Thus, one oxygen atom from each SO_2 unit of dithionite is proposed to coordinate to the Mo atom, thereby forming a bidentate complex (Figure 7). In this complex, the dithionite oxygen atoms are in hydrogen bond contact to the peptide nitrogen of Asp^{572} and the peptide oxygen and nitrogen of Met^{357}. As dithionite sulfur atoms have a weaker electron density than those of the dithiolene group, the occupancy of the dithionite was estimated to be about 50%. Therefore, crystallographic refinement was achieved with both the dithionite and the oxo and water ligands of the native

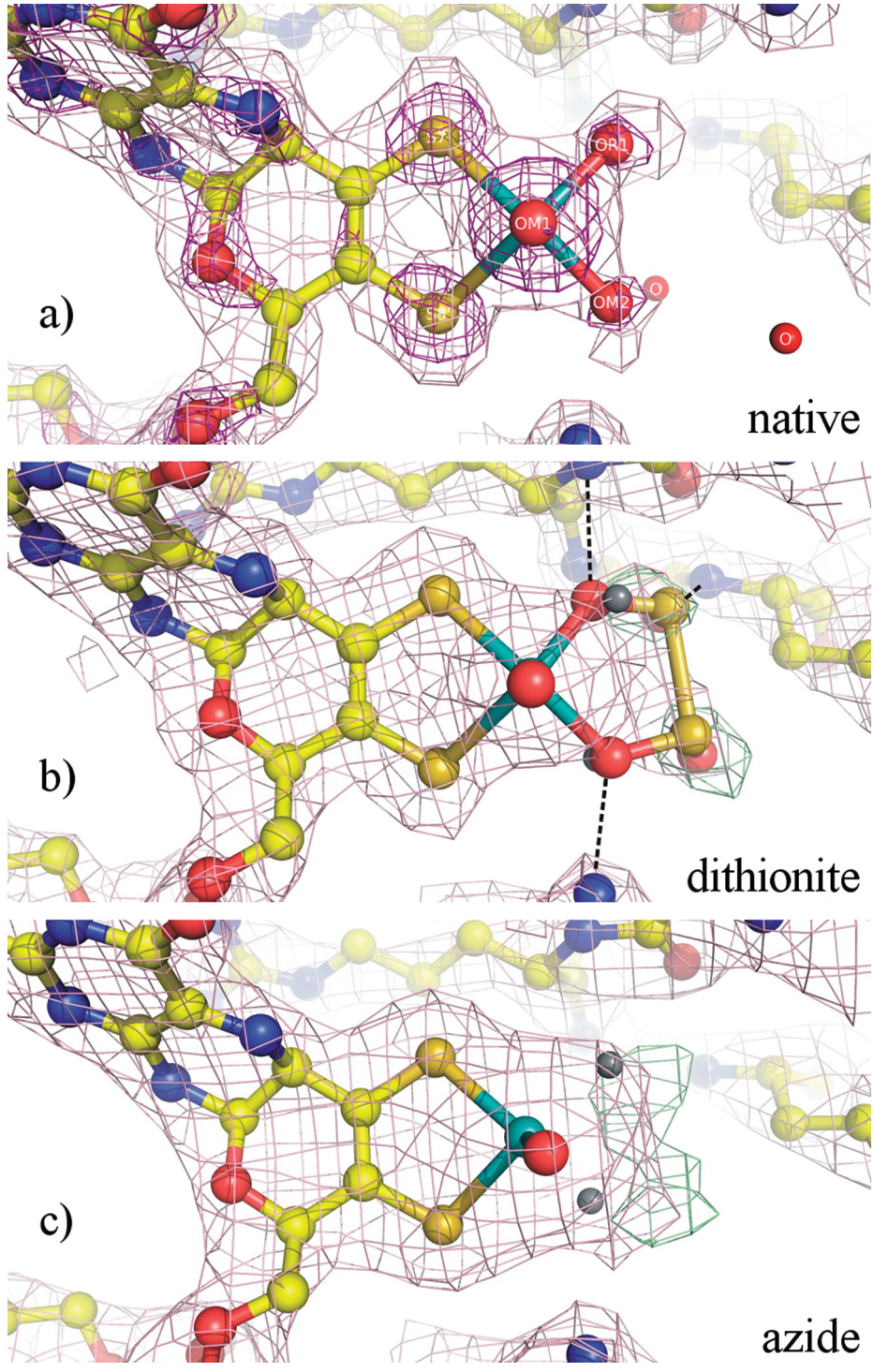

FIGURE 7: Mo ligation found in structures of 4-HBCR soaked with dithionite and azide. (a) Native structure of 4-HBCR$_{ox}$ showing the ligation pattern of Mo. The contour level of the electron density map was 3σ (in red) and 1.5σ (in light red). (b, c) 4-HBCR$_{dit}$ structure with dithionite and azide modeled as indicated. In both cases, the $2F_o - F_c$ and $F_o - F_c$ electron density maps (in light red and green) were calculated without dithionite (b) and without azide (c). Their contour levels were 1.5σ and 3σ, respectively. In ca. 50% of the active sites of the 4-HBCR$_{dit}$ and the 4-HBCR$_{az}$ crystals the Mo atom is equatorially coordinated by an oxo and a water ligand (as indicated by the gray balls).

structure as equatorial ligands. The electron density of the 4-HBCR$_{az}$ structure indicated azide binding on a significant level, but its profile did not allow to model it unambiguously into the ligation sites of the equatorial oxygen positions. A bidentate binding of the terminal nitrogen atoms of azide is excluded due to geometrical reasons. We suggest that azide preferentially occupied the coordination site of the water molecule, thereby ligating with one terminal nitrogen atom to Mo whereas the others point to the substrate binding site.

In summary, multiple modeling trials of dithionite and azide to the active site led to the result as presented (Figure 7). Nevertheless, other binding modes cannot be excluded. Due to the limited availability of appropriate enzyme crystals not all effectors could be investigated. In the case of sulfide

no soaking trials could be performed, as sulfide exhibited only a reactivating effect during turnover of 4-OH-BCoA. However, addition of 4-OH-BCoA resulted in an immediate dissolving of the crystals.

DISCUSSION

Active Site of 4-HBCR. The recently solved crystal structure of 4-HBCR at 1.6 Å resolution enabled initial insights into the structure/function relationship of 4-HBCR. However, no evidence for the presence of a sulfur ligand at the Mo atom was obtained, as this ligand was most possibly lost during the very long crystallization time of 5–6 weeks at 25 °C (*14, 26*). The loss of a sulfo or sulfido ligand during crystallization trials has also been reported for other XO members (*34, 35*). The results obtained in this work provide evidence that the Mo atom of 4-HBCR indeed contains a sulfur ligand: (i) cyanide inactivation is a typical feature of XO family members with a concomitant removal of the sulfur ligand from the Mo atom, (ii) 4-HBCR$_{ox/cn}$ can only be reactivated in the presence of sulfide, and (iii) the Mo(V) EPR signal of 4-HBCR$_{cn}$ in D_2O was highly similar to desulfo signals obtained with other XO family members and is therefore also referred to as a desulfo-inhibited signal. The Mo(V) signal of 4-HBCR$_{cn}$ in H_2O was more difficult to compare with those of other enzymes of the XO family as the signal in the isolated state was a mixture of inhibited/noninhibited states of 4-HBCR. The observed hyperfine splitting is interpreted as interactions of the Mo(V) species with two protons derived from a water and/or sulfido ligand.

In spite of the indirect evidence for the presence of a sulfur ligand at the Mo atom, some unusual properties of 4-HBCR with respect to sulfur atom removal and sulfur atom incorporation remain. These features comprise, e.g., the inability to determine thiocyanate from 4-HBCR$_{ox/cn}$ or the strict dependency of 4-HBCR$_{ox/cn}$ reactivation by sulfide on 4-OH-B-CoA turnover. An explanation for the latter phenomenon might be that sulfide can only bind to an intermediate state that occurs during substrate turnover. Soaking of 4-HBCR crystals with 4-OH-BCoA readily dissolved them, which suggests that major conformational changes occur upon substrate binding (*14*). As a consequence, it was also impossible to incorporate the proposed sulfur ligand to the Mo atom by simple crystal soaking experiments. Another unusual feature is that reactivation by sulfide does not yield a stable, active form of 4-HBCR as removal of excess sulfide converted the enzyme back into an inactive state. Thus, cyanide appears not only to remove the assumed sulfur ligand from the active site but also to alter the enzyme in a way that its sulfide-dependent conversion to an active form is no more stable.

Inhibiting Electron Donors. 4-HBCR was inactivated by dithionite and titanium(III) citrate in differing modes. To our knowledge nothing is known about the sensitivity of other XO family members toward these compounds. Inactivation by titanium(III) citrate is irreversible, but surprisingly, 4-HBCR$_{az}$ is largely protected from titanium(III) citrate inhibition. The protective effect of azide is assigned to its direct binding to the Mo atom (Figure 7). In contrast, the natural high-affinity ligand 4-OH-BCoA appears to replace azide readily from the Mo atom as azide has no inhibitory effect. Thus, we suggest the following order of binding affinities to 4-HBCR: 4-OH-BCoA > azide > titanium(III) citrate.

The reversible inhibitory effect of dithionite described here may explain the observed differing specific activities in individual enzyme preparations of 4-HBCR and may also necessitate investigators to reinterpret individual data obtained with other XO family enzymes in the presence of high dithionite concentrations. Dithionite was found to be coordinated directly to the Mo atom in the absence of the natural substrate by occupying the two variable equatorial positions of the square-pyramidal coordination sphere (the other two are fixed by the dithiolene sulfur atoms of the cofactor; Figure 7). This finding apparently suggests that dithionite replaces both the water and the assumed sulfur ligand at the Mo atom. However, as dithionite inhibition can be reversed by simple oxidation in the absence of sulfide ions, the Mo-bound sulfur atom should not be released from the enzyme by dithionite. A likely explanation is that the mode of dithionite binding as observed in the soaked crystals is only possible in the desulfo state of 4-HBCR.

Surprisingly, there was no significant difference in the Mo(V) EPR spectra of the dithionite, titanium(III) citrate, or methyl viologen reduced states of 4-HBCR. The most likely reason is that the inhibitory effect of dithionite and titanium(III) citrate is only exerted during substrate turnover and that the inhibitor binds only to an intermediate, diamagnetic state during catalysis, which escapes EPR detection. This assumption is supported by the observation that also the reactivation by sulfide is only achieved during substrate turnover. The time dependence of dithionite/titanium(III) citrate inhibition suggests that 4-HBCR is converted in a rather slow process into dithionite and/or titanium(III) citrate susceptible states.

Azide. In this work azide was shown to exhibit no inhibitory effect on 4-HBCR, which is in contrast to results from a previous study (*5*). A possible explanation for this discrepancy is that in the previous study inhibition assays were carried out in the presence of dithionite, possibly to protect 4-HBCR from oxygen damage. Thus, the observed inhibition may be explained by an effect of dithionite. Nevertheless, this work has shown that azide indeed binds directly to the Mo atom, probably by replacement of the water ligand, but obviously not in one defined conformation. The observation that azide binding prevented inhibition by titanium(III) citrate but not by dithionite can be explained by differing affinities to the Mo atom.

Cyanide. One of the most typical features of XO family enzymes is their sensitivity to cyanide which is accompanied by the release of a Mo-bound sulfur ligand as thiocyanate (*10, 19*). In many cases cyanide-inhibited members of the XO family can be reactivated in the presence of sulfide. However, the mode of inactivation and reactivation by sulfide largely depends on the reaction conditions and type of enzyme. 4-HBCR has properties similar to those of xanthine dehydrogenase from chicken liver with respect to the mechanism of cyanide inactivation (*19*). The two enzymes are inactivated in both the oxidized and reduced states. In the reduced state only the cyanide-inhibited 4-HBCR and xanthine dehydrogenase can simply be reactivated by oxidation; in contrast,

in the oxidized state all cyanide-inhibited XO family enzymes appear to be reactivated by high concentrations of sulfide (*19*).

ACKNOWLEDGMENT

We are grateful to the staff of the ID14 and ID29 beamlines, ESRF, Grenoble, for help during data collection.

REFERENCES

1. Boll, M., and Fuchs, G. (2005) Unusual reactions involved in anaerobic metabolism of phenolic compounds. *Biol. Chem. 386*, 989–997.
2. Boll, M., Fuchs, G., and Heider, J. (2002) Anaerobic oxidation of aromatic compounds and hydrocarbons. *Curr. Opin. Chem. Biol. 6*, 604–611.
3. Diaz, E. (2004) Bacterial degradation of aromatic pollutants: a paradigm of metabolic versatility. *Microbiology 7*, 173–180.
4. Gibson, J., and Harwood, C. S. (2002) Metabolic diversity in aromatic compound utilization by anaerobic microbes. *Annu. Rev. Microbiol. 56*, 345–369.
5. Brackmann, R., and Fuchs, G. (1993) Enzymes of anaerobic metabolism of phenolic compounds. 4-Hydroxybenzoyl-CoA reductase (dehydroxylating) from a denitrifying *Pseudomonas* species. *Eur. J. Biochem. 213*, 563–571.
6. Breese, K., and Fuchs, G. (1998) 4-Hydroxybenzoyl-CoA reductase (dehydroxylating) from the denitrifying bacterium *Thauera aromatica*—prosthetic groups, electron donor, and genes of a member of the molybdenum-flavin-iron-sulfur proteins. *Eur. J. Biochem. 251*, 916–923.
7. Boll, M., Fuchs, G., Meier, C., Trautwein, A., El Kasmi, A., Ragsdale, S. W., Buchanan, G., and Lowe, D. J. (2001) Redox centers of 4-hydroxybenzoyl-CoA reductase, a member of the xanthine oxidase family of molybdenum-containing enzymes. *J. Biol. Chem. 276*, 47853–47862.
8. Breese, K., Boll, M., Alt-Morbe, J., Schagger, H., and Fuchs, G. (1998) Genes coding for the benzoyl-CoA pathway of anaerobic aromatic metabolism in the bacterium *Thauera aromatica*. *Eur. J. Biochem. 256*, 148–154.
9. Brondino, C. D., Romao, M. J., Moura, I., and Moura, J. J. (2006) Molybdenum and tungsten enzymes: the xanthine oxidase family. *Curr. Opin. Chem. Biol. 10*, 109–114.
10. Hille, R. (1996) The mononuclear molybdenum enzymes. *Chem. Rev. 96*, 2757–2816.
11. Hille, R. (2005) Molybdenum-containing hydroxylases. *Arch. Biochem. Biophys. 433*, 107–116.
12. Boll, M. (2005) Key enzymes in the anaerobic aromatic metabolism catalysing Birch-like reductions. *Biochim. Biophys. Acta 1707*, 34–50.
13. Buckel, W., and Keese, R. (1995) One-electron redox reactions of CoASH esters in anaerobic bacteria—a mechanistic proposal. *Angew. Chem., Int. Ed. 34*, 1502–1506.
14. Unciuleac, M., Warkentin, E., Page, C. C., Boll, M., and Ermler, U. (2004) Structure of a xanthine oxidase-related 4-hydroxybenzoyl-CoA reductase with an additional [4Fe-4S] cluster and an inverted electron flow. *Structure 12*, 2249–2256.
15. Okamoto, K., Matsumoto, K., Hille, R., Eger, B. T., Pai, E. F., and Nishino, T. (2004) The crystal structure of xanthine oxidoreductase during catalysis: implications for reaction mechanism and enzyme inhibition. *Proc. Natl. Acad. Sci. U.S.A. 101*, 7931–7936.
16. Bonin, I., Martins, B. M., Purvanov, V., Fetzner, S., Huber, R., and Dobbek, H. (2004) Active site geometry and substrate recognition of the molybdenum hydroxylase quinoline 2-oxidoreductase. *Structure 12*, 1425–1435.
17. Huber, R., Hof, P., Duarte, R. O., Moura, J. J., Moura, I., Liu, M. Y., LeGall, J., Hille, R., Archer, M., and Romao, M. J. (1996) A structure-based catalytic mechanism for the xanthine oxidase family of molybdenum enzymes. *Proc. Natl. Acad. Sci. U.S.A. 93*, 8846–8851.
18. Brondino, C. D., Rivas, M. G., Romao, M. J., Moura, J. J., and Moura, I. (2006) Structural and electron paramagnetic resonance (EPR) studies of mononuclear molybdenum enzymes from sulfate-reducing bacteria. *Acc. Chem. Res. 39*, 788–796.
19. Coughlan, M. P., Johnson, J. L., and Rajagopalan, K. V. (1980) Mechanisms of inactivation of molybdoenzymes by cyanide. *J. Biol. Chem. 255*, 2694–2699.
20. Biegert, T., Altenschmidt, U., Eckerskorn, C., and Fuchs, G. (1993) Enzymes of anaerobic metabolism of phenolic compounds. 4-Hydroxybenzoate-CoA ligase from a denitrifying *Pseudomonas* species. *Eur. J. Biochem. 213*, 555–561.
21. Möbitz, H., and Boll, M. (2002) A Birch-like mechanism in enzymatic benzoyl-CoA reduction: a kinetic study of substrate analogues combined with an ab initio model. *Biochemistry 41*, 1752–1758.
22. Westley, J. (1981) Thiosulfate: cyanide sulfurtransferase (rhodanese). *Methods Enzymol. 77*, 285–291.
23. Hunt, J., and Massey, V. (1992) Purification and properties of milk xanthine dehydrogenase. *J. Biol. Chem. 267*, 21479–21485.
24. Otwinowski, Z., and Minor, W. (1996) Processing of X-ray diffraction data collected in oscillation mode. *Methods Enzymol. 276*, 307–326.
25. Bailey, S. (1994) The CCP4 Suite—programs for protein crystallography. *Acta Crystallogr. 50*, 760–763.
26. Unciuleac, M., Boll, M., Warkentin, E., and Ermler, U. (2004) Crystallization of 4-hydroxybenzoyl-CoA reductase and the structure of its electron donor ferredoxin. *Acta Crystallogr. 60*, 388–391.
27. Murshudov, G. N., Vagin, A. A., and Dodson, E. J. (1997) Refinement of macromolecular structures by the maximum-likelihood method. *Acta Crystallogr. 53*, 240–255.
28. Jones, T. A., Zou, J. Y., Cowan, S. W., and Kjeldgaard, M. (1991) Improved methods for building protein models in electron density maps and the location of errors in these models. *Acta Crystallogr. A 47* (Part 2), 110–119.
29. Emsley, P., and Cowtan, K. (2004) Coot: model-building tools for molecular graphics. *Acta Crystallogr. 60*, 2126–2132.
30. Wahl, R. C., and Rajagopalan, K. V. (1982) Evidence for the inorganic nature of the cyanolyzable sulfur of molybdenum hydroxylases. *J. Biol. Chem. 257*, 1354–1359.
31. Bray, R. C. (1988) The inorganic biochemistry of molybdoenzymes. *Q. Rev. Biophys. 21*, 299–329.
32. Bray, R. C., George, G. N., Gutteridge, S., Norlander, L., Stell, J. G., and Stubley, C. (1982) Studies by electron-paramagnetic-resonance spectroscopy of the molybdenum centre of aldehyde oxidase. *Biochem. J. 203*, 263–267.
33. Gutteridge, S., Tanner, S. J., and Bray, R. C. (1978) Comparison of the molybdenum centres of native and desulpho xanthine oxidase. The nature of the cyanide-labile sulphur atom and the nature of the proton-accepting group. *Biochem. J. 175*, 887–897.
34. Rebelo, J., Macieira, S., Dias, J. M., Huber, R., Ascenso, C. S., Rusnak, F., Moura, J. J., Moura, I., and Romao, M. J. (2000) Gene sequence and crystal structure of the aldehyde oxidoreductase from *Desulfovibrio desulfuricans* ATCC 27774. *J. Mol. Biol. 297*, 135–146.
35. Rebelo, J. M., Dias, J. M., Huber, R., Moura, J. J., and Romao, M. J. (2001) Structure refinement of the aldehyde oxidoreductase from *Desulfovibrio gigas* (MOP) at 1.28 Å. *J. Biol. Inorg. Chem. 6*, 791–800.

BI800137V